Heliyon 9 (2023) e21161

Contents lists available at ScienceDirect

Heliyon

journal homepage: www.cell.com/heliyon

Bacopa monnieri: A promising herbal approach for neurodegenerative disease treatment supported by *in silico* and *in vitro* research

Shehla Shoukat [a,b,*], Muhammad Amir Zia [b], Muhammad Uzair [b], Kotb A. Attia [c], Asmaa M. Abushady [d,e], Sajid Fiaz [f], Shaukat Ali [b,**], Seung Hwan Yang [g,***], Ghulam Muhammad Ali [h]

[a] *Department of Plant Genomics and Biotechnology, PARC Institute of Advance Studies in Agriculture Research, Affiliated with Quaid-e-Azam University, National Agriculture Research Centre, Islamabad, Pakistan*
[b] *National Institute for Genomics and Advanced Biotechnology, National Agriculture Research Centre, Islamabad, Pakistan*
[c] *Department of Biochemistry, College of Science, King Saud University, P.O. Box 2455, 11451, Riyadh, Saudi Arabia*
[d] *Biotechnology School, Nile University, 26th of July Corridor, Sheikh Zayed City, Giza, 12588, Egypt*
[e] *Department of Genetics, Agriculture College, Ain Shams University, Cairo, Egypt*
[f] *Department of Plant Breeding and Genetics, University of Haripur, 22620 Haripur, Pakistan*
[g] *Department of Biotechnology, Chonnam National University, Yeosu, 59626, Republic of Korea*
[h] *Pakistan Agriculture Research Council, Islamabad, Pakistan*

ARTICLE INFO

Keywords:
Bacopa monnieri
Bacopaside X
Neurodegeneration
Acetylcholinesterase inhibitors
Memory loss and anxiety
Inhibition activity

ABSTRACT

Neurodegenerative disorders, caused by progressive neuron loss, are a global health issue. Among the various factors implicated in their pathogenesis, dysregulation of acetylcholinesterase activity has been recognized as a key contributor. Acetylcholinesterase breaks down the neurotransmitter acetylcholine, important for neural transmission. Evaluating phyto-compounds from *Bacopa monnieri* Linn. through *in vitro* and *in silico* analysis may expand their role as alternative therapeutic agents by modulating the function of acetylcholinesterase and complementing existing treatments. To accomplish this objective, chemical structures of phyto-compounds were retrieved from PubChem database and subjected to *in silico* and *in vitro* approaches. Virtual screening was performed through molecular docking and molecular dynamic simulation resulting in four top hit compounds including quercetin, apigenin, wogonin, and bacopaside X (novel lead compound for acetylcholinesterase inhibitor) with least binding score. Further, dose dependent acetylcholinesterase inhibition biochemical assay depicted that bacopaside X, apigenin, quercetin, and wogonin exhibited strong potential against acetylcholinesterase with IC_{50} values of 12.78 μM, 13.83 μM, 12.73 μM and 15.48 μM respectively, in comparison with the donepezil (IC_{50}: 0.0204

Abbreviations: Acetylcholinesterase, (AChE); micromole, (μM); Inhibition concentration, (IC50); Alzheimer's disease, (AD); Acetylcholine, (ACh); Food and Drug Administration, (FDA); Acetylcholinesterase Inhibitors, (AChEIs); butyryl-cholinesterase, (BChE); Bacopa monnieri, (B. monnieri); Root mean square deviation, (RMSD); General Amber Force Field, (GAFF); Molecular operating Environment, (MOE); acetyl-thiocholine iodide, (AChI); Blood Brain Barrier, (BBB); Optimized Potentials for Liquid Simulations, (OPC).

* Corresponding author. Department of Plant Genomics and Biotechnology, PARC Institute of Advance Studies in Agriculture Research, Affiliated with Quaid-e-Azam University, National Agriculture Research Centre, Islamabad, Pakistan.
** Corresponding author.
*** Corresponding author.
E-mail addresses: f_shehla@yahoo.com (S. Shoukat), ymichigan@jnu.ac.kr (S.H. Yang).

https://doi.org/10.1016/j.heliyon.2023.e21161
Received 18 April 2023; Received in revised form 12 October 2023; Accepted 17 October 2023
Available online 20 October 2023

μM). The *in silico* and *in vitro* research suggests that *B. monnieri* phyto-compounds have the potential to modulate molecular targets associated with neurodegenerative diseases and have a role in neuroprotection.

1. Introduction

Neurodegenerative ailments are the miscellaneous group of genetic conditions resulting from the loss of function and structure of neurons. Relatively, in old age individuals about 60–80 % of the total mental illness is due to neurodegenerative disease mainly Alzheimer's disease (AD) [1]. Neurodegenerative diseases affect the brain and its functions mainly through neuronal loss, accumulation of protein aggregates, inflammation and oxidative stress, neurotransmitter imbalance, and loss of neuroprotective mechanisms [2]. In the United States alone about 5.5 million patients accounts of AD [3]. Cognitive issues, personality changes, low thinking processes, and abnormal behavior are the vital signs of AD [4]. Early medical symptoms include having trouble remembering people's names, events, discussions, short-term memory loss, alternate moods, and inability to understand [5]. As disease advances, late health conditions become more prominent like disorientation and ultimately difficulty in eating and walking [6]. Data available regarding AD showed that cholinergic neuron-rich region deterioration are linked with memory loss and anxiety [7].

Acetylcholine (ACh) has considerably linked with learning and memory functions [5–7]. Several drug classes have been approved by the United States Food and Drug Administration (FDA), the most important class is Acetylcholinesterase Inhibitors (AChEIs) [8]. The cholinergic system has a major role in the harmonization of learning and memory main mechanisms [9]. Both acetylcholinesterase (AChE) and butyryl-cholinesterase (BChE) have a role in amyloid beta (Aβ) aggregation during the pre-phase of amyloid plaque development [10]. Subsequently, AChE and BChE inhibition led to an increase in the ACh in the brain resulting in a reduction of plaque synthesis. As BChE and AChE are very similar in structure and function and involves in ACh hydrolysis, however, inhibiting peripheral BChE results in severe side effects. Hence researchers have a keen interest in developing selective AChEIs to cope with these side effects [11]. FDA approved drugs based on AChEIs *i.e.*, donepezil, tacrine, galantamine, and rivastigmine are being used for the treatment of AD but these drugs have limited efficacy for AD control. The major issues linked with these drugs are cholinergic adverse effects including muscle cramps, nausea, hepatoxicity, eczema rash, unfamiliar weakness, disturbance in the gastrointestinal track, etc. Therefore, developing more potent and effective medicinal chemicals is necessary [12].

Plant-based natural products play an important role in bridging the therapeutic gaps in various human diseases while offering more promising pharmacological effects [13]. The plant based natural products are already considered as the memory and learning booster in the community. Many medicinal plants can decrease the symptoms of memory loss and AD by triggering and inhibiting various cascades of reactions at the molecular and cell levels, [14] few of these plants are *Salvia officinalis* [15], *Huperzia serrata* contains a compound huperzine as known for its cholinesterase inhibitor effect *i.e.*, it can increase the level of acetylcholine [16], and *Ginkgo biloba* extract has potential to improve cognitive function and memory [17]. *B. monnieri* also have cognitive-enhancing effects [18]. This cognitive function is due to the availability of secondary metabolites in medicinal plants. *B. monnieri* in sub-continent mainly in India and Pakistan known as brahmi, has been used for centuries in Ayurveda. It originates in tropical Asia and is currently widespread throughout the globe including the tropics and subtropics [19]. It is native to the wetlands of Pakistan, Australia, Europe, Africa, Asia, and North and South America [20]. This is the wild herb grown specifically in the potohar marshy regions of Pakistan. *B. monnieri* is a rich source of powerful compounds that have antioxidant effects like bacosides, the important bioactive compounds of this plant. Bioactive compounds from *B. monnieri* interfered with the dopamine and serotonergic systems, but its important molecular function concerns promoting neuron signaling. So far, characteristics of saponins of *B. monnieri* known as bacosides are thought to be responsible for the cognitive effects of this plant [21,22]. Biologically active compounds like saponins, flavonoids, terpenoids, and phenols are the major components of this herb. The presence of these compounds indicates the antioxidant activity of *B. monnieri*. Consequently, its use may prevent and treat age and neuro-related diseases [23]. Keeping in view, the present study was designed to study the potential of *B. monnieri* phyto-compounds in mitigating neurodegenerative diseases. The *in silico* and *in vitro* methods are used to screen and analyze the binding affinity of selected compounds' target proteins. Furthermore, the top-hit docked compounds were identified and checked for their stability via molecular dynamic simulation. The top hit and stable compounds are further validated through biochemical assay and dose dependent responses of these compounds are estimated. Our study aims to lay groundwork for further investigation, including *in vivo* and animal model trails, to estimate the therapeutic efficacy of and safety of identified compounds.

2. Materials and methods

2.1. Ligand collection

B. monnieri contains different class of biological active compounds *i.e.*, saponins, triterpenoid bacosaponins, and saponin glycosides. More than 100 bioactive phytochemicals of *B. monnieri* were selected from published literature and Dr. Duke's Phytochemical and Ethnobotanical Database (https://phytochem.nal.usda.gov/) [24] Table S1. All phytochemicals *B. monnieri* were retrieved from PubChem. The ligands 3D structures were retrieved from PubChem database in. mol format and converted into PDB format following Discovery Studio 2021 Client. For energy minimization MMFF94X force fields were applied to each ligand and uploaded to Molecular Operating Environment MOE database for docking procedure.

2.2. Protein preparation

3D co-crystallized structures of human AChE (PDB ID - 3ZLT), protein was retrieved from RCSB-PDB [25]. The protein energy was minimized using UCSF Chimera (http://www.cgl.ucsf.edu/chimera/). Before molecular docking, all heteroatom and water molecules were deleted, and the structure was optimized in PyMOL2. Missing residues were inserted using modeler software. The structure of the receptor protein was prepared in PyMOL2 prior to docking via Molecular operating Environment (MOE) [26].

The active sites of *AChE protein* were confirmed via a literature survey and further, MOE software's Site Finder tool was used to explore the potential binding residues and the electrostatic surface maps around these residues to depict docking sites. The compounds were docked at the peripheral active site (defined docking site) of *AChE* protein using MOE tools. We found the 10 best docked molecule poses using the triangular method, minimized them with the force fields refinement algorithm, and estimated binding energy while maintaining receptor molecule stiffness using generalized born solvation models. Classification of the top 12 docked phyto-chemicals were listed in Table 1. Binding energy, S-score function, and Root mean square deviation (RMSD) values were used to identify the top 3 compounds. Top poses were chosen for further analysis *i.e.*, interaction with the proteins, and molecular dynamic simulation. The docked complexes with the least binding energy were designated for 2D and 3D interaction studies in MOE and PyMOL2 software.

2.3. ADMET and drug-related properties

Molinspiration was used to predict the properties linked with bioactivity and drug, including Log P, molecular mass, hydrogen bond donors, hydrogen bond acceptor, PSA, Ro5 violations, and rotatable bonds. Log P values were used to predict the bioavailability of the drug molecules. Molinspiration data for the number of rotatable bonds, number of H-bond donors, and acceptors were evaluated by Lipinski's rule of five. This rule explains about molecules that can cross the membrane have hydrogen bond acceptors $\leq$10, hydrogen bond donor's $\leq$ 5, and molecular weight $\leq$500. The metabolism, distribution, absorption, toxicity (ADMET), and excretion properties were also analyzed using the SwissADME server [27].

This work used combined approach *i.e.*, computational, and *in vitro* methods to investigate the possible AChE inhibitory action of *B. monnieri* phyto-compounds. We intended to combine these two methods to better understand the chemicals' interactions with the AChE enzyme. This combination strategy also lays the groundwork for *in vivo* research to evaluate the drugs' efficacy, safety, and therapeutic potential.

2.4. Molecular docking

The pocket residues of the protein were identified via literature survey and also confirmed from site finder tools of MOE to investigate the anionic sub active site of AChE and generate electrostatics surface maps around the residues to describe binding sites within docking.

Docking of selected compounds against protein within the defined docking site, MOE software was utilized. By using of triangular algorithm explored the best poses between docked molecules and London DG function and force fields minimized 10 postures generated through docking [28] and binding energies were obtained, whereas, maintained the receptor residues inflexible through generalized born solvation models [29]. Based on binding energy, S-score function, and Root-Mean-Square-Deviation (RMSD), top compounds were calculated from docking analysis. The ligands were chosen for other analyses like molecular dynamic simulation and *invitro* AChE activity due to their energies as well as their interaction within the active pocket of AChE protein.

Table 1
Phytochemicals associated with *Bacopa monnieri*.

Sr. No	CompoundS	Class	SMILES
1	Apigenin	Flavonoids	O1c2c(C(=O)C=C1c1ccc(O)cc1)c(O)cc(O)c2
2	Luteolin	Flavonoids	O1c2c(C(=O)C=C1c1cc(O)c(O)cc1)c(O)cc(O)c2
3	Quercetin	Flavonol	O1c2c(C(=O)C(O)=C1c1cc(O)c(O)cc1)c(O)cc(O)c2
4	Bacosterol	Glycoside	OC1CC2CCC3C(=CCC(C)C(CC=C3)C(CCC(C(C)C)CC)C)C2(CC1)C
5	Brahmic acid/ madecassic acid	Triterpenoid saponin	OC1C(C2C(C3CC=C4C5C(C)C(CCC5(CCC4(C)C3(CC2O)C)C(O)=O)C)(CC1O)C)(CO)C
6	Oroxindin	Phenolic	OC1C(C2C(C3CC=C4C5C(C)C(CCC5(CCC4(C)C3(CC2O)C)C(O)=O)C)(CC1O)C)(CO)C
7	Stigmasterol	Stigmastanes	O1C(C(O)=O)C(O)C(O)C(O)C1Oc1cc(O)c2c(OC(=CC2=O)c2ccccc2)c1OC
8	Wogonin	Flavone	OC1CC2=CCC3C4CCC(C(C=CC(C(C)C)CC)C)C4(CCC3C2(CC1)C)C
9	Bacoside A	Triterpenoid saponins	O1c2c(C(=O)C=C1c1ccccc1)c(O)cc(O)c2OC
10	Bacoside B	Triterpenoid saponins	O1C(CO)C(OC2OCC(O)C(O)C2O)C(O)C(O)C1OC1CCC2(C(CCC3(C2CCC2C3(CC(=O)C2C(O)(CCC=C(C)C)C)C)C1(C)C)CO
11	Bacoside I	Triterpenoid saponins	O1C(CO)C(OC2OCC(O)C(O)C2O)C(O)C(O)C1OC1CCC2(C(CCC3(C2CCC2C3(CC(=O)C2C(O)(CCC=C(C)C)C)C)C1(C)C)CO
12	Bacopaside X	Triterpenoid saponins	S(OCC1OC(OC2C(OC3OC(CO)C(O)C3O)C(OCC2O)OC2CCC3(C(CCC4(C3CCC3C45CC4(OCC(C=C(C)C)C(O)(C34)C)OC5)C)C2(C)C)C)C(O)C(O)C1O)(=O)(=O)[O-]

2.5. Ligand receptor interaction analysis

The interaction study of docked complexes was carried out in a substantial way by employing the MOE's ligX tool to create 2D illustrations of receptor ligand interactions highlighting the formation of hydrogen bonds, electrostatic/non-electrostatic interactions, and hydrophobic bonds [30]. MD trajectory analysis was performed on the top 3 docking HITS compounds.

2.6. Molecular dynamic simulation of the protein ligands complexes

The interaction behaviors seem highly convincing when the associated proteins are examined inside a dynamic context. We generated the complexes via MoE software and further subjected them to molecular dynamic simulation, initial files were prepared through General Amber Force Field (GAFF) using LEap module and antechamber packages using semi empirical method *i.e.*, bcc approach of Amber 20. So, we also employed a molecular modeling technique utilizing AMBER20 software to analyze the influence of ligands 1–3 *i.e.* quercetin, apigenin and bacopaside X binding towards molecules [31]. Prior to MD-simulation FF14SB force fields were applied to the system, OPC (Optimized Potentials for Liquid Simulations) water model was used, and all complexes were neutralized as well through Na + ions. Other algorithms used for molecular dynamic simulations are as: combined the steepest descent and conjugate gradient strategies, approximately 9000 steps of minimization were accomplished, which comprised 6000 steps during the initial iteration and 3000 steps throughout the 2nd stages. The temperature for heating the system was adjusted at 300 K, and individual protein-ligands complexes were allowed to equilibrate for 10ns. Additionally, the final steps of the MD production run were performed at 50ns using CUDA. Trajectory analysis was performed via CPPTRAJ module [32]. The below formula has been performed for investigation of the root means square deviation (RMSD) with respect to time assessing structural stability.

$$\mathrm{RMSD} = \Sigma\ \mathrm{d2i} = 1\ \mathrm{N\ atoms}\ \sqrt{}$$

where these di signifies the changes among atom positions while I indicate the underlying and superimposed architecture of the structure. The root mean square fluctuation (RMSF) is calculated based on the B-factor that represents the main crucial limitation for calculating the overall flexibility of amino acids inside a protein. The RMSF may be obtained analytically by employing the underneath formula:

$$\text{Thermal factor or B - factor} = [(8\pi * * 2) / 3]\ (\mathrm{msf})$$

The MM/PBSA. py package has been used to predict the binding free energy of complexes [33]. The free energy of every complex was determined by anticipating individual energy components, such as van der Waals energy (vdW), electrostatic energy, polar and non-polar solvation energies, and was extensively employed throughout numerous researches. Every complex's entire trajectory (10, 000 frames) was incorporated in this study. Using the equation below, the energy components have been computationally analyzed to establish each system's net binding free energy:

$$''\Delta G \text{ net binding energy}'' = ''\Delta G \text{ complex binding energy}''$$
$$- [\,''\Delta G \text{ receptor binding energy}'' + ''\Delta G \text{ ligand binding energy}'']''$$

Each of the above components of net binding energy can be split as follows:

$$''G'' = ''G \text{ bonded}'' + ''G \text{ van der Waals}'' + ''G \text{ polar solvation energy}'' + ''G \text{ non-polar solvation energy}''$$

Entropy was not measured, because of it has been time-consuming and high cost that is also prone to major mistakes.

2.7. Biochemical analysis

For biochemical analysis, the top hit compounds were purchased from Sigma Aldrich, Germany *i.e.*, the bacopaside X analytical grade (Cat No: 42488), quercetin (Product No. 337951), apigenin (Product No. 10798) and wogonin (Product No. W0769).

2.7.1. Invitro AChE activity of top hit ligands

The Ellman spectrophotometric procedure was used to check the inhibitory effect of 4 top hit compounds with AChE enzyme from *Electrophorus electricus* (electric eel) (Sigma-aldrich (Product No. C2888) [34]. 100 μL Tris – HCl buffer (1 M, pH 8.0), 50 μL5, 5′-dithio-bis (2-nitro-benzoic) acid (DTNB), and 50 μL AChE (5.32 × 10-3 U) kept at 30 °C and shake for 15 min. In the end, the reaction was started with the addition of 50 μL of acetyl-thiocholine iodide (AChI) used as a substrate. The enzyme inhibition was recorded spectrophotometrically at 412 nm and then the IC_{50} value was calculated. The effect of various concentrations of phytocompounds was screened against AChE at ranges (0.25–400 μM) and for donepezil (0.25–400 nM). The AChE inhibitory effect for concentration (0.25, 2, 12.5, 25, 50, 100, 200 and 400) μM was estimated. The IC_{50} was then calculated from the % inhibition graph for each extract using Originlab 8.1 software.

3. Results and discussion

In this study, a few of the phytochemicals that have inhibition properties for target proteins linked with AD from the medicinal plant *B. monnieri* were identified. Grid box for these 12 compounds were based on docking into AChE and was set around Trp 86 [35]. The selected phytocompounds showed effective binding affinities and the least binding energies with the target protein. However, the docking patterns of all ligands are separately discussed in Table 2. AChE revealed binding affinity with all 12 compounds but minimum

binding energies were observed with bacopaside X, apigenin, quercetin, wogonin, and oroxindin. This has been justified with the obtained binding energies *i.e.*, −17.87, −16.71, −16.53, 15.56 and −15.05 Å kcal/mol. Oroxindin and wogonin showed almost the same binding energies.

The strength and stability during enzyme and inhibitor complex formation can be evaluated by the number of hydrogen bonds (H-bonds) formed between them. Apigenin makes five hydrogen bonds with AChE amino acid residues namely, Tyr-72 (2.78), Tyr-124 (3.49/1.83), Ser-293 (1.9), and Trp-286 (1.99) Å (Fig. 1A). Bacopaside X form four hydrogen bond with mentioned bond distances Tyr-72 (2.83), Tyr-124 (2.94/2.28), and Trp-286 (2.18) Å (Fig. 1B). Quercetin also forms five hydrogen bonds in active site Thr-75, Try-124, Arg-296, Trp-286, and Ser-293 with a bond distance of (3.09, 3.43, 1.91, 2.91, and 2.72) Å, respectively (Fig. 1C). Wogonin forms two hydrogen bonds with AChE amino acids Arg-296 (2.53 and 2.95 Å). Oroxindine forms three hydrogen bonds with amino acids residues of AChE *i.e.*, Tyr-72 (1.94 Å), Arg-296 (1.94 Å), Ser-93 multiple hydrogen bonds of (2.81; 2.94) Å. Apart from making hydrogen bonds these ligands also show Van der waals and hydrophobic interactions with other amino acid residues of the active site as depicted in Table 2. Oroxindin and wogonin showed almost the same binding energies.

3.1. Binding stability and rigidity of the docking complex

The three top hit protein ligand complexes showed stable conformations on molecular dynamic simulation analyses.

3.2. Root mean square deviation (RMSD)

At 50 ns, enzyme-ligand conformational dynamics were assessed. The root means square deviation plot for acetyl cholinesterase and apigenin complex revealed variability at 5 ns and 23.5 ns with a maximum deviation of 1.91 Å Fig. 2a. The quercetin-complex RMSD ranged from 0.50 to 1.85 Å. Fig. 2b shows that the RMSD plot for the complex of acetyl cholinesterase and quercetin showed maximum fluctuations up to 17 ns and then became steady after 17 ns. The RMSD values for both the protein and the ligand were between 0.45 and 1.9 Å, which means that the complex was stable. At 19 and 47 ns, the RMSD for the acetyl cholinesterase

Table 2
Molecular Docking and Interaction analysis of selected phyto-compounds of *Bacopa monnieri* with AChE.

S. No	Ligands	Hydrogen (H) bonds and distance	Hydrogen Distance (Å)	Van der waals and Hydrophobic Interaction	Energy (kCal/mol)
1	Apigenin	Tyr-72 Tyr-124 Trp-286 Ser-293	2.78 3.49/1.83 1.99 1.9	Leu-289, Leu-76, Asp-74, Thr-75, Tyr-341, Arg-296, Phe-338	−16.71
2	Luteolin	Tyr-124	3.49	Try-286, Tyr-341, Ser-293, Glu-292, Asp-74, Phe338, Tyr-72, Gln-291	−13.45
3	Quercetin	Thr-75 Try-124 Trp-286 Arg-296 Ser-293	3.09 3.43 2.91 1.91 2.72	Phe-297, Trp-286, Phe-336, Tyr-341, Tyr-72, Asp-74, Leu-76, Ile-294, Phe-295,	−16.53
4	Bacosterol	Leu-289	3.03/2.6	Tyr-72, Phe-338, Tyr-124, Phe-297, Tyr-341, Ile-294, Arg-296, Gln-291, Ser-293, His-287, Glu-292, Val-288, Phe-295	−10.45
5	Brahmic Acid	–		His-287, Trp-286, Tyr-72, Phe-338, Tyr-124, Tyr-341, Gln-291, Ser-293, Leu-289, Glu-292	−13.52
6	Oroxindin	Tyr-72 Arg-296 Ser-93	1.94, 1.94, 2.81/2.94	Phe-297, Tyr-341, Trp-286, Tyr-124,Phe-338, Ser-125, Asp-74, Val-73, Asn-87, Ile-294, Leu-289, Phe-295, Gln-291	−15–05
7	Stigmasterol	–		Tyr-341, Phe-338, Trp-286, Asp-74, Tyr-124, Tyr-72, His-287, Asp-283	−11.48
8	Wogonin	Arg-296	2.53/2.95	Phe-295, Tyr-341, Tyr-124, Phe-338, Trp-286, Tyr-72, Ile-294, Leu-289, Phe-297, Ser-293	−15.56
9	Bacoside A	Tyr-337 Leu-339 Tyr-341	1.32 1.33 3.01	Ser-336, Val-340, Ile-294, Phe-295, Phe-297	−12.47
10	Bacoside B	Tyr-337 Leu-339 Tyr-341	1.32 1.33 3.01	Ser-336, Val-340, Ile-294, Phe-295, Phe-297	−12.47
11	Bacoside I	Tyr-337 Leu-339 Tyr-341	1.32 1.33 3.01	Ser-336, Val-340, Ile-294, Phe-295, Phe-297	−11.37
12	Bacopaside X	Tyr-72 Tyr-124 Trp-286	2.83 2.94/2.28 2.18	Trp-86, Asp-74, His-297, Leu-289, Val-288, Glu-292, Phe-297, Gln-291, Arg-296, Phe-338, Try-337	−17.87
13	Donepezil (Reference Drug)	Tyr-155, Trp-286 Glu-313	2.18 3.01 2.92	Thr-238, Thr-311, Pro-312, Gly-234, Gln-291, Gln-413, Asn-317, Arg-493 Asn-533, Pro-537, Arg-417	−8.16

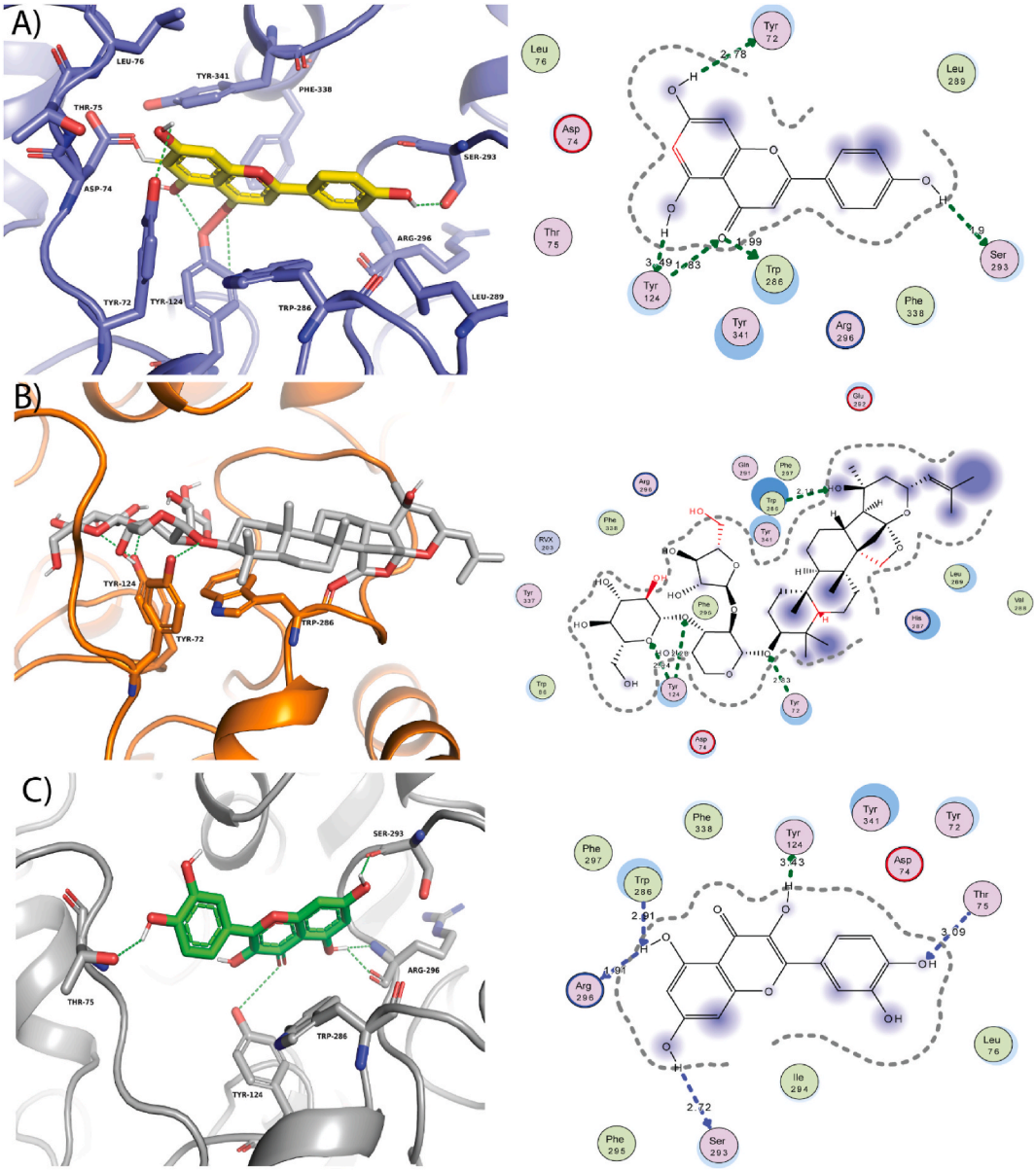

Fig. 1. Interaction of potential lead compounds of BM with the ACHE protein. (A) Apigenin (Yellow), (B) Bacopaside X (Grey), (C) Quercetin (Green). Ligands are shown as sticks. Hydrogen bonds between the receptor and ligands are shown as green dotted lines along with 2D structure complex.

complex with bacopaside X was substantially different from the average, but after that, it became more stable Fig. 2c.

Root-mean-square fluctuation (RMSF).

RMSF peaks calculate the protein area where residues fluctuate more during simulation. Fig. 3 shows complex RMSF peaks. To assess protein system flexibility, the RMSF of each amino acid residue was estimated during simulation. Acetyl cholinesterase complexes had RMSFs of 0.4–2.5 Å and 0.5 to 4.5 Å, with local ligand-contact maxima of 2.7, 2.9, and 4 Å for apigenin, quercetin, and Bacopaside X, respectively Fig. 3. During simulation, atoms showed stable and acceptable RMSF fluctuations. These findings suggest that these proteins and their ligands form a stable combination.

Radius of gyration (Rg) and Hydrogen bonds.

The radius of gyration (Rg) is used to analyze protein structural equilibrium during simulation. Fig. 4a, b and 4c showed the Rg values of the acetylcholinesterase-apigenin complex, acetylcholinesterase-quercetin complex, andacetyl cholinesterase-bacopaside X complex during the MD trajectory poses, respectively. The simulation at 50 ns yielded Rg values of 0.15 ± 0.36 nm, 0.24 nm ± 0.21 nm, 0.25 nm ± 0.22 nm, and 0.34 nm ± 0.31 nm, respectively. Fig. 5a, b and 5c showed the hydrogen bond formation in bound and unbound state for acetylcholinesterase-apigenin complex, acetylcholinesterase-quercetin complex, and acetylcholinesterase-

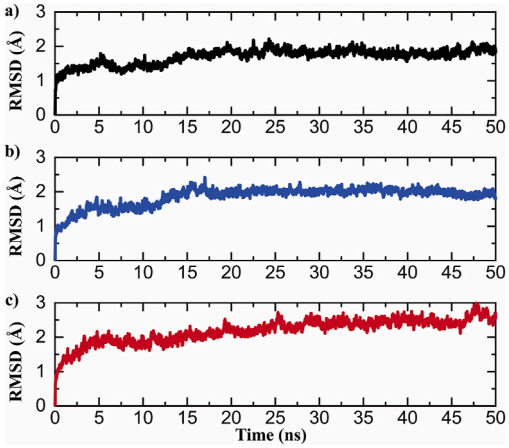

Fig. 2. Root Mean square deviation (RMSD) of three protein ligand complexes (a) AChE-apigenin complex, (b) AChE-quercetin complex (c) AChE-bacopaside-X complex.

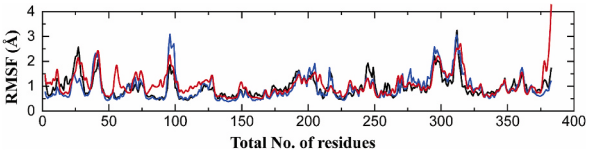

Fig. 3. Root-mean-square fluctuation (RMSF) of three protein ligand complexes (a) AChE-apigenin complex, (b) AChE-quercetin complex (c) AChE-bacopaside-X complex.

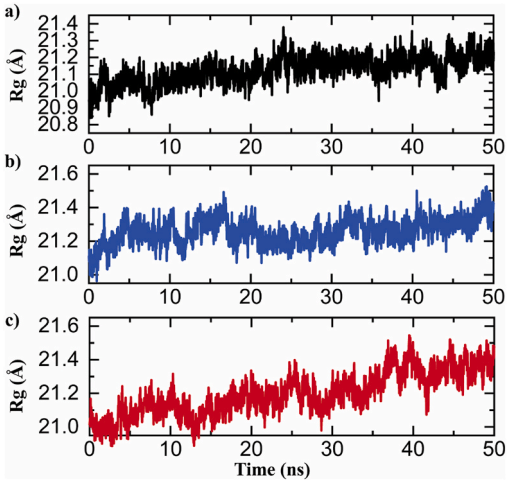

Fig. 4. Radius of gyration (Rg) of three protein ligand complexes (a) AChE-apigenin complex, (b) AChE-quercetin complex (c) AChE-bacopaside-X complex.

bacopaside X complex during the MD trajectory pose, respectively.

3.3. Docking score vs. MMPBSA analyses

Binding and dissociation are two crucial stages in ligand-protein interactions, which are essential for the performance of biological tasks. The binding affinity between two systems increases as the duration between the two events increases. Studies of protein-ligand interactions shed light on the molecular details of ligand binding and release from the active site. This study contributes to our understanding of the importance of specific amino acids in the inhibitor's binding to the protein as a whole. In the current study, molecular docking was used to find out how the ACHE protein and its powerful inhibitors from the *B. monnieri* plant interact structurally.

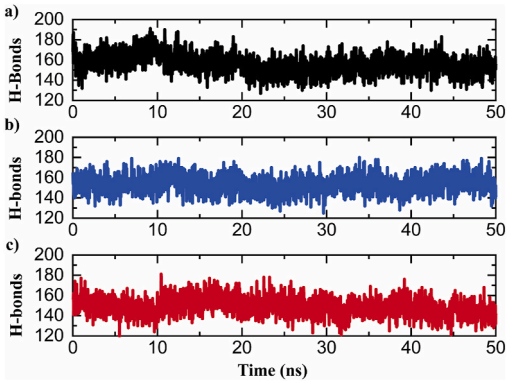

Fig. 5. Hydrogen Bond of three protein ligand complexes (a) AChE-apigenin complex, (b) AChE-quercetin complex (c) AChE-bacopaside-X complex.

The binding affinity of top 12 phytochemicals was enlisted in Table 2. Among these top three compounds apigenin (1A), quercetin (1Q) and bacopaside X (BX) showed highest binding affinity toward ACHE protein. These three complexes were then used for were then used as a starting structure in MD simulation studies. These AChE-apigenin complex, AChE-quercetin complex, and AChE-bacopaside-X complexes served as the initial structures for molecular dynamics (MD) simulation research. Binding affinity can be determined using docking studies, however, the time-evolved behavior of the ligand within the active pocket provides a more complete picture of ligand motion. The AChE-apigenin complex, AChE-quercetin complex, and AChE-bacopaside-X complexes binding affinities were calculated using the semiquantitative MMPBSA method. It has been shown that the Molecular Mechanics Poisson-Boltzmann Surface Area (MMPBSA) method for calculating binding free energy are the most popular means of calculating interaction energies and are frequently used to investigate biomolecular complexes. Based on Docking and MMPBSA calculations, the ligands have high binding energy. AChE-bacopaside-X complex depicted −51.40 kcal/mol turn out to be the best binder for AChE in terms of binding energy as predicted by molecular docking results coupled with MMPBSA method followed by AChE-quercetin complex (−35.81 kcal/mol) and AChE-apigenin complex (−32.65 kcal/mol) (Table 3). The MM/PBSA computation confirmed the docking score ranking of bacopaside X as having the highest negative binding free energy compared to its competitors.

3.4. *In vitro AChE inhibitory activities of phytochemicals*

The top hit phytochemicals of *B. monnieri* were further analyzed for anti-AChE activity. The spectrophotometric assay for AChE was performed using minor modification in Ellman's protocol [34]. At the concentration of 100 μM, bacopaside X, quercetin, apigenin and wogonin possessed 87 %, 85.7 %, 80 % and 80.3 % AChE inhibition, respectively, as compared to the donepezil (89 %) (Fig. 6). Further, concentration dependent acetylcholinesterase inhibition biochemical assay depicted that bacopaside X, apigenin, quercetin, and wogonin exhibited strong potential against AChE with IC_{50} values of 12.78 μM, 13.83 μM, 12.73 μM and 15.48 μM respectively, in comparison with the donepezil (IC_{50}: 0.0204 μM) Fig. 7A–E. Nonlinear regression analysis depicted that the Log IC_{50} values for bacopaside X was 1.106 ± 0.019 μM as compared to donepezil (0.01302 ± 0.024 μM). AChE inhibition showed that bacopaside X was more bioactive than donepezil ($p < 0.0001$).

Molecular docking, molecular dynamics simulations, and biochemical experiments reveal how *B. monnieri* phyto-compounds interact with AChE to decrease its enzymatic activity. The identified interactions help explain the chemical mechanisms behind the drugs' therapeutic benefits. Our findings are in line with the previously reported study of aporphine derivate provision the aforesaid idea *i.e.*, inhibition via anionic subactive site of AChE [35]. Another idea linked with the mechanism, as noncompetitive inhibitors bind

Table 3
Binding Free energy of three protein ligand complexes AChE-apigenin complex, (b) AChE-quercetin complex (c) AChE-bacopaside-X complex.

Parameters	1A (MM-PBSA)	1Q (MM-PBSA)	BX (MM-PBSA)
VDWAALS	−37.45 ± 0.16	−42.30 ± 0.26	−74.41 ± 0.29
EEL	−7.68 ± 0.18	−12.34 ± 0.20	250.08 ± 0.99
EGB	15.79 ± 0.15	23.16 ± 0.15	−219.31 ± 0.84
ESURF	−3.31 ± 0.01	−4.33 ± 0.01	−7.75 ± 0.02
DELTA G gas	−45.13 ± 0.23	−54.64 ± 0.33	175.67 ± 1.02
DELTA G solv	12.48 ± 0.15	18.83 ± 0.15	−227.07 ± 0.85
DELTA TOTAL (kCal/mol)	**−32.65 ± 0.17**	**−35.81 ± 0.28**	**−51.40 ± 0.32**
Dock Score (kCal/mol)	**−16.71**	**−16.53**	**−17.87**

VDWAALS = van der Waals contribution from MM; EEL = electrostatic energy as calculated by the MM force field; EPB/EGB = the electrostatic contribution to the solvation free energy calculated by PB or GB respectively; ECAVITY = nonpolar contribution to the solvation free energy calculated by an empirical model; and DELTA G binding = final estimated binding free energy calculated from the terms above. (kCal/mol) = kilocalorie/mol; MM-PBSA= Molecular Mechanics Poisson-Boltzmann Surface Area.

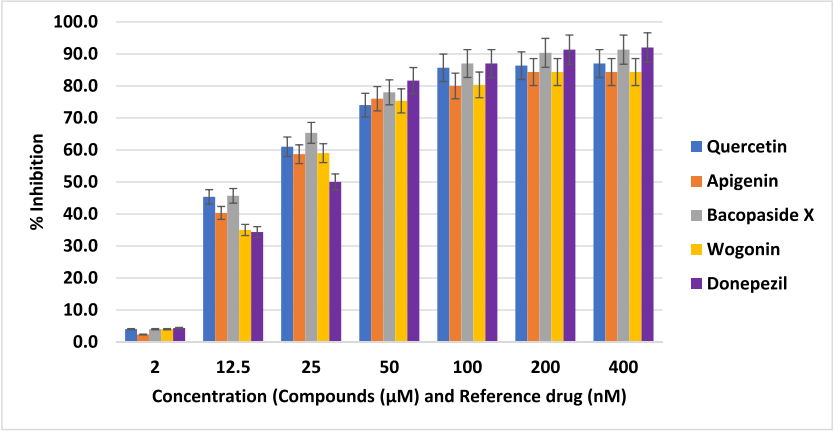

Fig. 6. *Invitro* AChE inhibitory activities of 4 top hit phytochemicals.

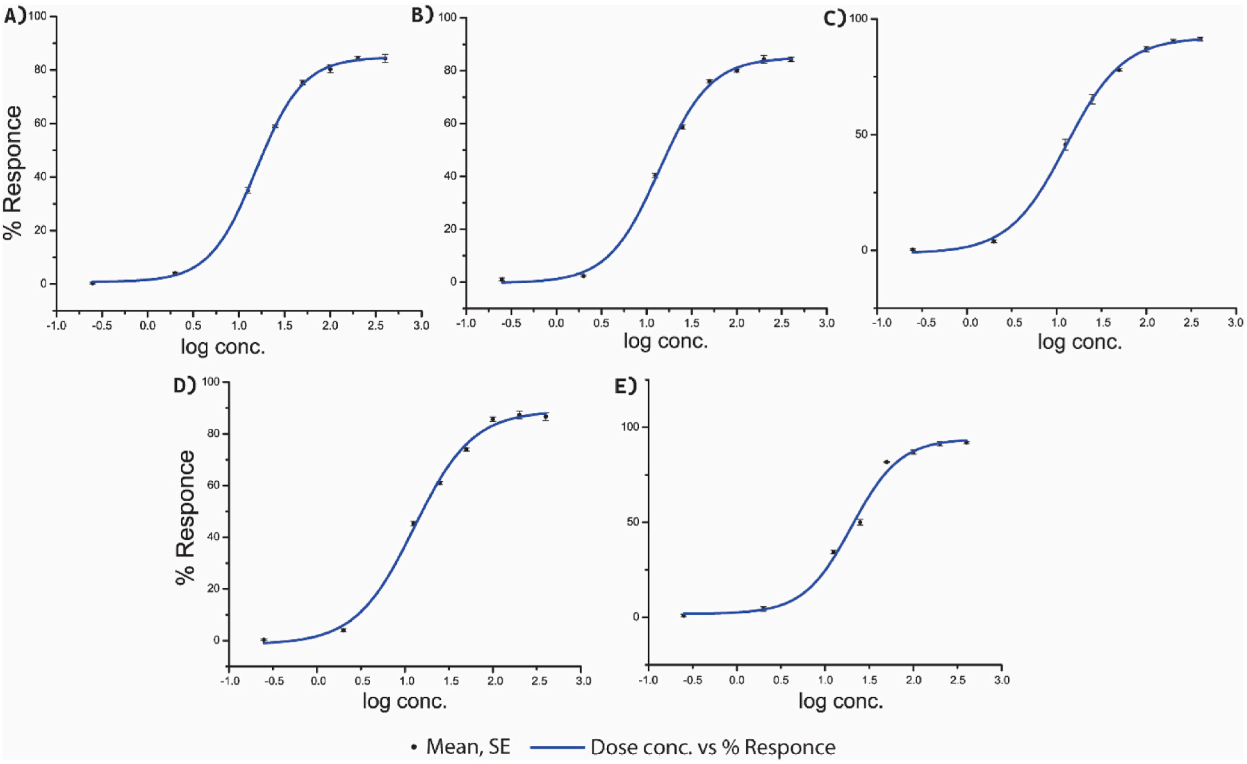

Fig. 7. Log dose response curve and IC_{50} of the four top hit compounds. A) Log dose quercetin B) Log dose wogonin C) Log dose apigenin D) Log dose bacopaside X and E) Log dose donepezil.

to the anionic subsite of the AChE enzyme just like market available drug donepezil and tacrine [36–38]. Some of the aphorphine and triterpenoid saponin derivatives have been reported to perform dual activity towards AChE *i.e.*, interact with anionic subsite along with peripheral anionic subsite [39,40]. Therefore, we evaluated the possible interaction and figured out that for apigenin H bond (1.9 A) between OH (Position 4) and Ser 293 stabilized by π-π interaction with Trp 286 Fig. 1A. Likewise, Tyr 72 makes hydrogen bonds with the OH group (Position 8). Try 286 and Tyr 124 to form hydrogen bonds with OH and O group (Position 5 and 4) with the distance of 1.83A and 1.99A and stabilized by π-π with Tyr 341. Bacopaside X form 3 bond with the anionic subsite of its sugar moiety and 1 hydrogen bond in its aglycone part of the compound. The hydrogen bonds formed at 3 different positions with Tyr-124, Tyr 72, and Trp 286 were stabilized by π – π interaction with Trp-86, Asp-74, His-297, Leu-289, Val-288, Glu-292, Phe-297, Gln-291, Arg-296, Phe-338, Try-337. Quercetin on the other hand makes 5 hydrogen bonds at (Position 3, 13, 15, and 18) with OH. Making it a more stable interacting compound with a bond distance less than 4 and stabilized by π – π interaction with Phe-297, Trp-286, Phe-336,

Tyr-341, Tyr-72, Asp-74, Leu-76, Ile-294, Phe-295. Facts about understudied 12 phytocompounds interaction with AChE are given in Table 2. The study of the compounds was prerequisite because the *B. monnieri* extract has been used widely for centuries in the subcontinent for cognition enhancement however, the mechanism is still unknown. The docking results are in line with the [35,41] in which the authors have reported the same amino acids interaction with the secondary metabolite "boldine" and enzyme AChE and BChE [42]. However, we try to figure out the *insilico* mechanism, and how the bioactive compounds of *B. monnieri* affect the cholinesterase activity [43]. Hydrogen bonding, hydrophobic contacts, and other non-covalent interactions generated persistent complexes with critical residues in the active site, preventing acetylcholine from reaching the catalytic site [35]. Besides this, the molecular dynamic study reveals the stability of complexes of the three top-hit compounds as reported earlier in various other studies [28]. These simulations revealed dynamic protein-ligand interactions. The phyto-compounds remained stable in the active site of AChE throughout the simulation, confirming their inhibitory activity. Phytocompounds inhibited AChE enzymatic action in *in vitro* biochemical studies. These experiments show dose-dependent suppression of acetylcholine hydrolysis, suggesting the drugs reduce AChE catalytic activity. This inhibition may enhance synaptic cleft acetylcholine levels, improving neurodegenerative disease cholinergic dysfunction.

Understanding how *B. monnieri* phyto-compounds target AChE can help treat neurological disorders. These substances may increase cholinergic neurotransmission by suppressing AChE [44]. Cholinergic deficiencies cause cognitive deterioration in neurodegenerative illnesses like AD [7]. Additionally, phytocompounds may protect the brain. These chemicals may have antioxidant, anti-inflammatory, or neurotrophic properties beyond AChE inhibition [45]. These mechanisms may enhance neurodegenerative disease treatment. Our study gives mechanistic insights, but more research is needed to completely understand the mechanisms of action of *B. monnieri* phyto-compounds and their effects *in vivo*. However, here are some potential limitations of Blood Brain Barrier (BBB) penetration for these compounds: molecular weight and size, lipophilicity and hydrophilicity, efflux transporters, metabolism and degradation, species differences. Therapeutic applications, especially those with brain-based target locations, need to be taken into account while considering the BBB penetration limitations of these chemicals. Chemical modifications, formulation approaches, co-administration with BBB-permeabilizing drugs, and different delivery modalities (e.g., nasal delivery, nanoparticles) are all possibilities for overcoming these restrictions and increasing CNS availability. Animal models and clinical trials are necessary to prove their efficacy, safety, and disease-modifying potential.

4. Conclusion

In conclusion, we found bacopaside X, a new lead drug with substantial AChE inhibition, through molecular docking and biochemical testing. Bacopaside X may regulate the cholinergic system, which is essential for learning and memory. Our findings also demonstrate the need for more robust neurodegenerative disease treatments. While useful, FDA-approved medications have limited efficacy and cholinergic side effects. *B. monnieri* phyto-compounds like bacopaside X may help develop alternative or complementary treatments that overcome these restrictions. The rationale for future exploration is strengthened as a result of the identification of bacopaside X as a top hit chemical through *in silico* analysis and its validation through *in vitro* studies. In order to evaluate the therapeutic potential of bacopaside X and its effectiveness in reducing the symptoms of neurodegenerative illnesses, additional research, including *in vivo* investigations and clinical trials, is required in the near future.

Data availability statement

Data used to support this study is given in supplementary file. The data associated with present study been not been deposited into any publicly available repository. All the data generated is within this manuscript any data will be made available upon request.

Funding statement

The authors are thankful to the National Institute of Genomics and Advanced Biotechnology, NARC, Islamabad, for providing a funding source to complete this study. This work was supported by National Research Foundation of Korea (NRF) grant funded by the Korean Government (MSIT) (NRF-2021R1F1A1055482).

CRediT authorship contribution statement

Shehla Shoukat: Writing – original draft, Methodology, Data curation, Conceptualization. **Muhammad Amir Zia:** Writing – original draft, Formal analysis, Data curation. **Muhammad Uzair:** Writing – review & editing, Methodology, Funding acquisition, Formal analysis. **Kotb A. Attia:** Writing – review & editing, Writing – original draft, Funding acquisition. **Asmaa M. Abushady:** Writing – review & editing, Funding acquisition. **Sajid Fiaz:** Writing – review & editing, Writing – original draft, Funding acquisition. **Shaukat Ali:** Project administration, Formal analysis, Data curation, Conceptualization, Supervision, Writing - review & editing. **Seung Hwan Yang:** Writing – review & editing, Funding acquisition. **Ghulam Muhammad Ali:** Resources, Methodology, Formal analysis, Conceptualization, Writing - review & editing.

Declaration of competing interest

All authors have direct intellectual contribution to the manuscript. The authors are in complete agreement to make submission with

Heliyon. The authors declare no conflict of interest.

Acknowledgements

The authors extend their appreciation to the Researchers Supporting Project number (RSP-2024R369), King Saud University, Riyadh, Saudi Arabia. This work was supported by National Institute of Genomics and Advanced Biotechnology, NARC, Islamabad.

Appendix A. Supplementary data

Supplementary data to this article can be found online at https://doi.org/10.1016/j.heliyon.2023.e21161.

References

[1] G.M. Babulal, et al., Associations between homelessness and Alzheimer's Disease and related Dementia: a systematic review, J. Appl. Gerontol. 41 (11) (2022) 2404–2413.
[2] E.A. Ayeni, et al., Neurodegenerative diseases: implications of environmental and climatic influences on neurotransmitters and neuronal hormones activities, Int. J. Environ. Res. Publ. Health 19 (19) (2022), 12495.
[3] T.J. Saleem, et al., Deep learning-based diagnosis of Alzheimer's Disease, J. Personalized Med. 12 (5) (2022) 815.
[4] A. Terracciano, A.R. Sutin, Personality and Alzheimer's disease: an integrative review, Personality Disorders: Theory, Research, and Treatment 10 (1) (2019) 4.
[5] J.G. Goldman, S.K. Holden, Cognitive syndromes associated with movement disorders, Continuum: Lifelong Learning in Neurology 28 (3) (2022) 726–749.
[6] S. Weintraub, Neuropsychological assessment in dementia diagnosis, Continuum: Lifelong Learning in Neurology 28 (3) (2022) 781–799.
[7] Z.-R. Chen, et al., Role of cholinergic signaling in Alzheimer's disease, Molecules 27 (6) (2022) 1816.
[8] G. George, et al., Structural modifications on chalcone framework for developing new class of cholinesterase inhibitors, Int. J. Mol. Sci. 23 (6) (2022) 3121.
[9] A. Salehipour, et al., Combination therapy in Alzheimer's disease: is it time? J. Alzheim. Dis. (2022) 1–17 (Preprint).
[10] J.G. Fernández-Bolaños, Ó. López, Butyrylcholinesterase inhibitors as potential anti-Alzheimer's agents: an updated patent review (2018-present), Expert Opin. Ther. Pat. 32 (8) (2022) 913–932.
[11] B.T. Tung, et al., Molecular docking and molecular dynamics approach to identify potential compounds in Huperzia squarrosa for treating Alzheimer's disease, J. Compl. Integr. Med. 19 (4) (2022) 955–965.
[12] D. Padhi, T. Govindaraju, Mechanistic insights for drug repurposing and the design of hybrid drugs for Alzheimer's Disease, J. Med. Chem. 65 (10) (2022) 7088–7105.
[13] R.E. Aluko, Food-derived acetylcholinesterase inhibitors as potential agents against Alzheimer's Disease, eFood 2 (2) (2021) 49–58.
[14] M.B. Dick, et al., The variability of practice hypothesis in motor learning: does it apply to Alzheimer's disease? Brain Cognit. 44 (3) (2000) 470–489.
[15] N. Babault, et al., Acute effects of Salvia supplementation on cognitive function in athletes during a fatiguing cycling exercise: a randomized cross-over, placebo-controlled, and double-blind study, Front. Nutr. 8 (2021) 949.
[16] A.G. Zaki, et al., Microbial acetylcholinesterase inhibitors for Alzheimer's therapy: recent trends on extraction, detection, irradiation-assisted production improvement and nano-structured drug delivery, Appl. Microbiol. Biotechnol. 104 (11) (2020) 4717–4735.
[17] R. Das, et al., Ginkgo biloba: a treasure of functional phytochemicals with multimedicinal applications, Evid. base Compl. Alternative Med. (2022) 2022.
[18] E.A. Walker, M.V. Pellegrini, Bacopa Monnieri, StatPearls Publishing, 2023 in StatPearls [Internet].
[19] P.S. Shankar, et al., Brahmi (Bacopa monnieri) as functional food ingredient in food processing industry, J. Pharmacogn. Phytochem. 7 (3) (2018) 189–194.
[20] R. Lansdown, S. Knees, A. Patzelt, Bacopa monnieri. The IUCN red list of threatened species 2013: e. T164168A17722668, 2013.
[21] H. Singh, et al., Effect of bacosides A and B on avoidance responses in rats, Phytother Res. 2 (2) (1988) 70–75.
[22] B. Dhawan, H. Singh, Pharmacological studies on Bacopa monniera, an Ayurvedic nootropic agent, Eur. Neuropsychopharmacol (6) (1996) 144.
[23] H. Singh, B. Dhawan, Neuropsychopharmacological effects of the ayurvedic nootropic bacopa monniera linn.(brahmi), Indian J. Pharmacol. 29 (5) (1997) 359.
[24] C. Lans, T. van Asseldonk, Dr. Duke's Phytochemical and Ethnobotanical Databases, a Cornerstone in the Validation of Ethnoveterinary Medicinal Plants, as Demonstrated by Data on Pets in British Columbia, Medicinal and Aromatic Plants of North America, 2020, pp. 219–246.
[25] J. Cheung, et al., Structures of human acetylcholinesterase in complex with pharmacologically important ligands, J. Med. Chem. 55 (22) (2012) 10282–10286.
[26] F.A. Alhumaydhi, Integrated computational approaches to screen gene expression data to determine key genes and therapeutic targets for type-2 diabetes mellitus, Saudi J. Biol. Sci. 29 (5) (2022) 3276–3286.
[27] L. Schrödinger, W. DeLano, PyMOL (2020).
[28] B. Ahmed, et al., Exploring multi-target inhibitors using in silico approach targeting cell cycle dysregulator–CDK proteins, J. Biomol. Struct. Dyn. 40 (19) (2022) 8825–8839.
[29] M. Tahir ul Qamar, et al., Computational screening of medicinal plant phytochemicals to discover potent pan-serotype inhibitors against dengue virus, Sci. Rep. 9 (1) (2019) 1–16.
[30] T. Joshi, et al., Structure-based screening of novel lichen compounds against SARS Coronavirus main protease (Mpro) as potentials inhibitors of COVID-19, Mol. Divers. 25 (2021) 1665–1677.
[31] T.-S. Lee, et al., Alchemical binding free energy calculations in AMBER20: advances and best practices for drug discovery, J. Chem. Inf. Model. 60 (11) (2020) 5595–5623.
[32] D.R. Roe, T.E. Cheatham III, PTRAJ and CPPTRAJ: software for processing and analysis of molecular dynamics trajectory data, J. Chem. Theor. Comput. 9 (7) (2013) 3084–3095.
[33] A.C. Timucin, Structure based peptide design, molecular dynamics and MM-PBSA studies for targeting C terminal dimerization of NFAT5 DNA binding domain, J. Mol. Graph. Model. 103 (2021), 107804.
[34] S.V. Shetab-Boushehri, Ellman's method is still an appropriate method for measurement of cholinesterases activities, EXCLI J 17 (2018) 798–799.
[35] A. Kostelnik, M. Pohanka, Inhibition of acetylcholinesterase and butyrylcholinesterase by a plant secondary metabolite boldine, BioMed Res. Int. 2018 (2018).
[36] M. Pohanka, Biosensors containing acetylcholinesterase and butyrylcholinesterase as recognition tools for detection of various compounds, Chem. Pap. 69 (1) (2015) 4–16.
[37] J.K. Marquis, Pharmacological significance of acetylcholinesterase inhibition by tetrahydroaminoacridine, Biochem. Pharmacol. 40 (5) (1990) 1071–1076.
[38] D.G. Wilkinson, The pharmacology of donepezil: a new treatment for Alzheimer's disease, Expet Opin. Pharmacother. 1 (1) (1999) 121–135.
[39] H. Tang, et al., Synthesis, biological evaluation and molecular modeling of oxoisoaporphine and oxoaporphine derivatives as new dual inhibitors of acetylcholinesterase/butyrylcholinesterase, Eur. J. Med. Chem. 44 (6) (2009) 2523–2532.
[40] S. Pecic, M.A. McAnuff, W.W. Harding, Nantenine as an acetylcholinesterase inhibitor: SAR, enzyme kinetics and molecular modeling investigations, J. Enzym. Inhib. Med. Chem. 26 (1) (2011) 46–55.
[41] Q. Jamal, et al., A computational study of natural compounds from bacopa monnieri in the treatment of alzheimer's disease, Curr. Pharmaceut. Des. 26 (7) (2020) 790–800.

[42] Q.M. Thai, et al., Searching for AChE inhibitors from natural compounds by using machine learning and atomistic simulations, J. Mol. Graph. Model. 115 (2022), 108230.
[43] Z. Yang, et al., Synthesis and structure–activity relationship of nuciferine derivatives as potential acetylcholinesterase inhibitors, Med. Chem. Res. 23 (2014) 3178–3186.
[44] V.N. Talesa, Acetylcholinesterase in Alzheimer's disease, Mechanisms of ageing and development 122 (16) (2001) 1961–1969.
[45] P. Wal, et al., Neuro-nutraceuticals: insights of experimental evidences and molecular mechanism in neurodegenerative disorders, Future Journal of Pharmaceutical Sciences 9 (1) (2023) 31.